Nanoindentation of Au and Pt/Cu thin films at elevated temperatures

Alex A. Volinsky[a)]
University of South Florida, Department of Mechanical Engineering, Tampa, Florida 33620
Neville R. Moody
Sandia National Laboratories, Livermore, California 94550
William W. Gerberich
University of Minnesota, Department of Chemical Engineering and Materials Science, Minneapolis, Minnesota 55455

(Received 24 March 2004; accepted 20 May 2004)

This paper describes the nanoindentation technique for measuring sputter-deposited Au and Cu thin films' mechanical properties at elevated temperatures up to 130 °C. A thin, 5-nm Pt layer was deposited onto the Cu film to prevent its oxidation during testing. Nanoindentation was then used to measure elastic modulus and hardness as a function of temperature. These tests showed that elastic modulus and hardness decreased as the test temperature increased from 20 to 130 °C. Cu films exhibited higher hardness values compared to Au, a finding that is explained by the nanocrystalline structure of the film. Hardness was converted to the yield stress using both the Tabor relationship and the inverse method (based on the Johnson cavity model). The thermal component of the yield-stress dependence followed a second-order polynomial in the temperature range tested for Au and Pt/Cu films. The decrease in yield stress at elevated temperatures accounts for the increased interfacial toughness of Cu thin films.

I. INTRODUCTION

The microelectronic industry has been growing rapidly over the past 10–20 years, as has its reliance on thin-film deposition techniques for components manufacturing. As modern devices generate quite a bit of heat, and peak temperatures can reach over 100 °C, there is a need to provide adequate cooling for a device to stay operable. Obviously these thermal cycles are unavoidable and eventually lead to thermal fatigue damage and device failure. Consequently, the knowledge of elastic and plastic properties of thin films at elevated temperatures is required for proper chip design and reliability assessments. For the proper stress analysis in conjunction with the thermal cycling characterization, it is important to measure the mechanical properties of thin films at elevated temperatures.

Nanoindentation is an alternative test method to the freestanding film mechanical testing[1] and microbeam cantilever deflection techniques[2,3] for measuring mechanical properties of thin films. First applied over 20 years ago in the hard-drive industry, it is now commonly used for microelectronic components and thin films. Nanoindentation is similar to conventional hardness tests, but nanoindentation is performed on a much smaller scale, using special equipment. The force required to press a sharp diamond indenter into the tested material is recorded as a function of indentation depth. Both elastic modulus and hardness can be readily extracted from the nanoindentation curve.[4–7] For a metal film, the yield stress (σ_{ys}), is often approximated as 1/3 of the hardness[8] measured by nanoindentation. Alternatively, it can be extracted from the extent of the plastic zone size around the indenter (c), measured by atomic force microscopy (AFM), using Johnson's spherical cavity model approach[9,10]

$$\sigma_{YS} = \frac{3P_{\max}}{2\pi c^2} \quad , \tag{1}$$

where P_{max} is the maximum indentation load. Although this expression was originally used for bulk materials, it was also shown to be applicable for thin films.[10]

In the case of a metal thin film, the yield stress is typically much higher than for a bulk material, because metal films are typically nanocrystalline. The dependence of yield stress on grain size is often described by a Hall-Petch type relationship

[a)] Address all correspondence to this author.
e-mail: volinsky@eng.usf.edu
DOI: 10.1557/JMR.2004.0331

 © 2004 Materials Research Society

$$\sigma_{YS} = \sigma_i + kd^{-n} \quad , \tag{2}$$

where σ_i is some intrinsic stress, independent of the grain size d; and n is between 0.5 and 1. The classic $1/d^{0.5}$ Hall-Petch relationship is not typically observed for thin films (due to substrate effects, limiting thin-film plasticity, or dislocation looping along the metal/oxide interface).[11]

If the grain size of a thin film is larger than the film thickness (t), the latter can be used instead of the grain size as a scaling parameter[12]

$$\sigma_{YS} = \alpha(1 + \beta t^{-1/2}) \quad , \tag{3}$$

where α and β are the fitting parameters. A similar approach, based on the film thickness, is used by Nix[11] to predict Cu flow-stress behavior.

Because hardness is known to decrease with temperature for bulk metals and single crystals,[13] similar effects are also expected in thin films. While conventional mechanical testing experiments are routinely performed in environmental chambers (and even in vacuum at high temperatures for bulk materials), nanoindentation experiments with thin films are challenging at elevated temperatures. Metallic thin films tend to oxidize, so the properties measured are more of the surface oxide, rather than of the metal film itself. Exceptions to this phenomenon are noble metals. One of the approaches for solving the surface-oxidation problem is to perform nanoindentation in ultra-high vacuum,[13–15] or inside an electron microscope (TEM).[16] Technically such tasks appear to be challenging though, because specialized equipment and sample preparation are necessary, and because some indenter parts are not vacuum-compatible.

Even without considering surface oxidation, the factor of thermal drift further complicates nanoindentation measurements. There have been three approaches undertaken to address this problem. First, placing the indenter tip assembly at a distance from the actuator, a strategy that allows indentation at temperatures as high as 500 °C.[17,18] Second, placing the whole indenter into the heated chamber.[19] Third, locally heating a very small sample and performing indentation after thermal equilibrium between the sample and the indenter tip has been reached; as well as accounting for thermal drift.[20] The authors have used the third approach to measure properties of thin Au and Cu films at temperatures from 20 to 130 °C, experimental aspects of which will be now considered.

II. EXPERIMENT

Local miniature heaters became commercially available with the development of AFM instrumentation.[21] For the high-temperature nanoindentation experiments, a resistance heating stage (Fig. 1) from Digital Instruments[21,22] was used in conjunction with a Nanoindenter II (using a 300-nm radius Berkovich diamond indenter). The heating accessory consisted of a sample heater and an electronic controller that allows for setting a desired temperature up to 130 °C with a 0.1 °C resolution. The heater is a ceramic block that contains an embedded resistive microheater. With a sample glued to a puck (using thermoepoxy), this assembly is then clamped onto the top of the microheater with the thermocouple (Fig. 1). The heating element is thermally isolated from the surrounding atmosphere so that it is mostly the sample surface that conducts heat into the atmosphere.

Initially, the thermocouple sample clamp did not provide enough mechanical force to clamp the steel puck to the heater. This failure resulted in sample movement during indentation. The clamp was modified; and for all further indentation experiments, the load-displacements curves obtained with the heater were checked to ensure absence of the sample motion or sliding. Also, elevated-temperature indentation experiments were performed on fused quartz.[23]

Thin Au and Cu films were RF sputter-deposited onto polished ⟨100⟩ silicon substrates to a nominal thickness of 3 μm, using a Perkin Elmer 2400 RF sputter system. A 15-s pre-sputter was used to prepare the surfaces. The system was pumped down to 1 μTorr, after which the thin films were deposited at a power of 1000 W. The

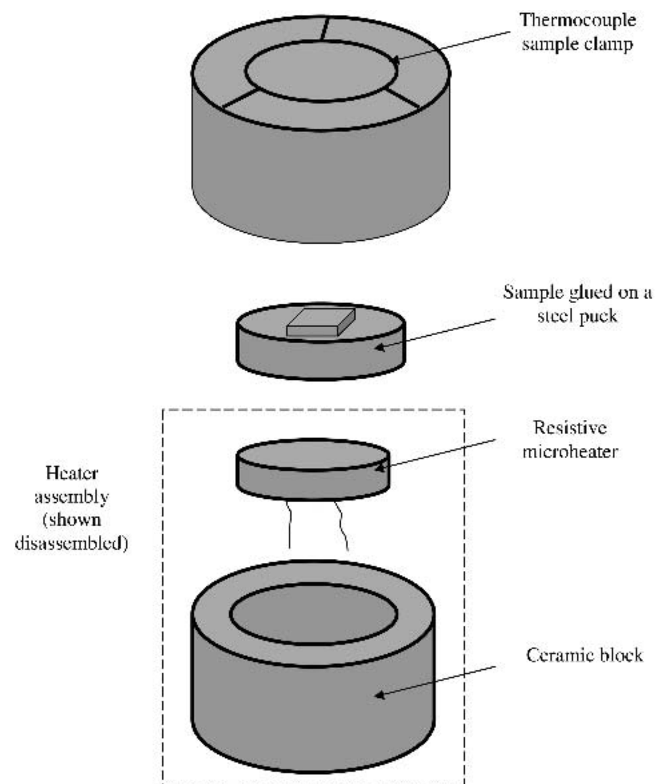

FIG. 1. Heater assembly components.

maximum temperature during the sputter process reached 100 °C; and for Cu films, the system was cooled down for 1 h after deposition to avoid film oxidation. Further/additional details of the deposition process are discussed elsewhere.[20,28,29] A sequence of increasing temperature indentations was performed on each sample, followed by room-temperature experiments to ensure that there were no annealing effects. Figure 2 shows load-displacement curves taken at room temperature (100 °C and 130 °C), and again at room temperature after all heating experiments. Both load-displacement curves performed at room temperature before and after heating are practically identical.

Continuous stiffness measurement was used for all indentation experiments with the modulation frequency of 45 Hz and a 2-nm displacement amplitude. The drift rate was measured during a 100-s hold following unloading to 10% of the maximum indentation load. As seen in Fig. 3, there is about a 120-nm sample movement due to the thermal drift and possibly creep at a constant load of 25 mN in 100 s. Continuous stiffness measurements of both elastic modulus and hardness accounted for thermal drift by using the tip-contact area corresponding to the drift-corrected indentation depth. Elevated-temperature nanoindentation experiments were also performed on fused quartz to ensure that no artifacts were present. The fused-quartz elastic modulus reduced to 69 GPa at 120 °C, compared to 72 GPa at room temperature.[23]

Oxidation is the main obstacle for experiments evaluating constitutive properties, because a surface oxide has markedly different properties. Original nanoindentation

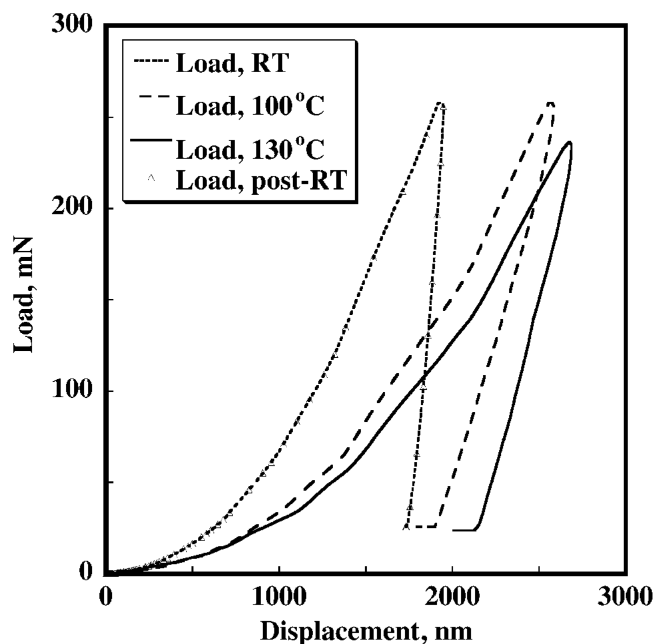

FIG. 2. Pt/Cu load-displacement curves obtained at room temperature, 100 °C and 130 °C.

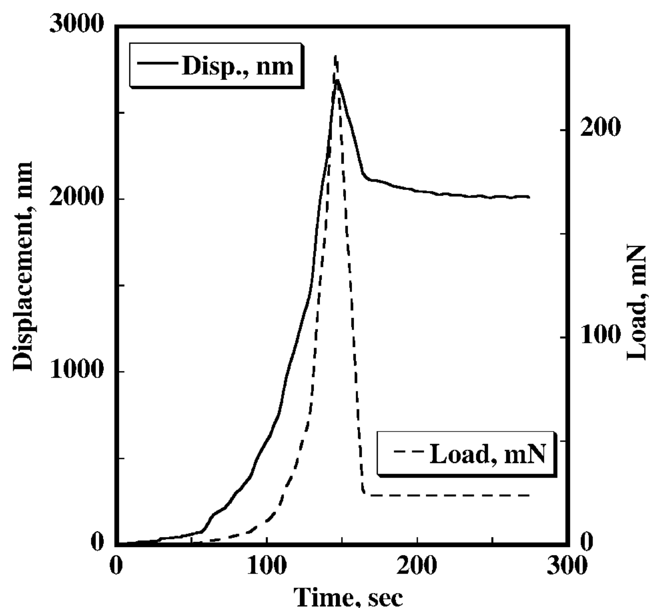

FIG. 3. Load and displacement profiles for a 130 °C indentation into Pt/Cu film.

experiments were first performed on the gold sputter-deposited films to avoid the oxidation effects observed in other metallic films. Nanoindentation tests were then performed on copper films (capped with a 5- to 10-nm platinum layer) at temperatures up to 130 °C. The platinum layer was deposited to prevent surface oxidation. Because the modulus and hardness values were taken at a depth much larger that the Pt layer thickness, and because Pt has a slightly higher elastic modulus (171 GPa) than Cu, it was assumed that a thin Pt layer did not affect the measurements of mechanical properties for Cu films at larger indentation depths.

III. DISCUSSION

The 2.7-μm gold film was indented at depths ranging from 20 nm to 2000 nm, at test temperatures from 20 °C to 130 °C. An apparent modulus drop with increased temperature is seen in Fig. 4 for the gold film. There appears to be a plateau in the modulus data at the shallow indentation depth, up to 100 nm, as shown in Fig. 5. At room temperature the modulus plateaus at about 90 GPa for a 100-nm indentation depth, and the modulus drops to 69 GPa at 130 °C (Fig. 5). Pt/Cu films exhibit a similar plateau modulus effect. Elastic-modulus plateau values and corresponding standard deviations for Au and Cu films are presented in Table I. Young's modulus depends on the composition, crystal structure, and orientation of the film material. Heat treatment has little effect on the modulus, so long as it does not affect the mentioned parameters. However, the Young's modulus for bulk materials at the melting point is typically between one-half

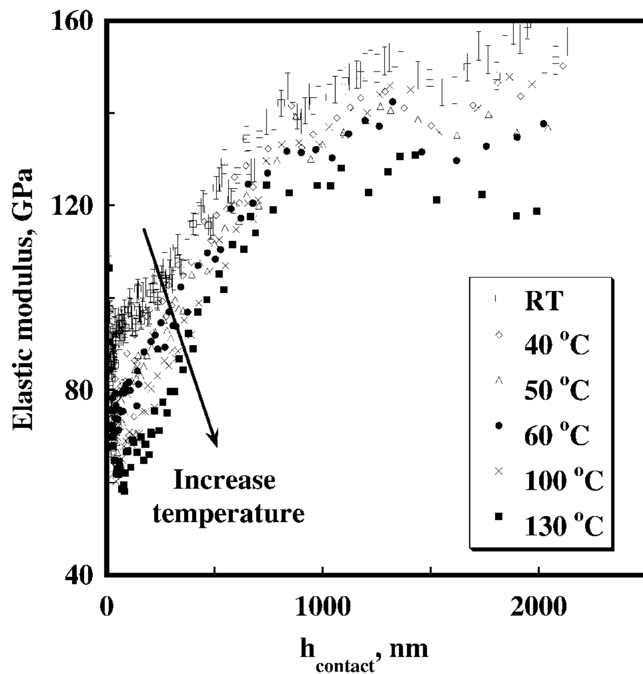

FIG. 4. Elastic modulus as a function of indentation depth for Au films at different testing temperatures.

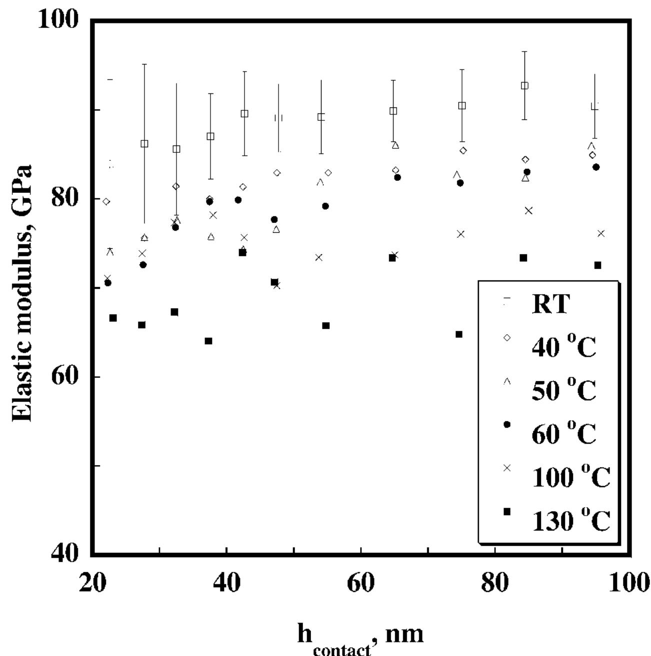

FIG. 5. Shallow indentation depth elastic modulus plateau region from Fig. 4.

to two-thirds the room-temperature value. At elevated temperatures, a modulus drop is expected due to thermal expansion and an increased amplitude of atomic vibrations. For example, for bulk Cu, a temperature increase of 200 °C leads to a 20 GPa decrease in modulus.[24] Elastic modulus temperature data for bulk Cu and Au[25,26] is also presented in Table I, for comparison. Although

TABLE I. Elastic properties of bulk and thin-film Au and Cu at elevated temperatures.

Temp. °C	Au film modulus/SD, GPa	Bulk Au modulus, GPa	Pt/Cu film modulus/SD, GPa	Bulk Cu modulus, GPa
20	88.6/4.9	80.7	123.4/8.28	131.7
40	82/6.8	80	122.3/7.57	131
50	79.4/7.4	79.7	···	130.3
60	78.8/6.2	79.4	110.2/7.89	129.8
100	75/11.7	78.1	103.1/8.91	127.4
130	69/13.6	76.4	90.56/7.46	125.7

not originally expected, the thermal drift-corrected elastic-modulus data in Table I shows that the temperature effect is more pronounced for nanocrystalline Au and Cu thin films, compared to the bulk Au and Cu.

Because plastic deformation is a thermally activated process, larger temperature effects on the film yield stress are expected. A 60% hardness drop is observed with the temperature increase up to 130 °C, as seen in Fig. 6 at shallow indentation depth. This temperature effect is not as pronounced at indentation depths over 500-nm, where the substrate hardness comes into play. In fact, the substrate effect becomes apparent at about a 200-nm contact depth, as the hardness increases due to a substrate effect. Similar to the elastic modulus data presented in Fig. 5, there appears to be a hardness plateau at a shallow indentation depth of 100-nm in Fig. 7. This initial plateau was used to estimate the true yield stress of Au as a function of test temperature (Fig. 8), using the

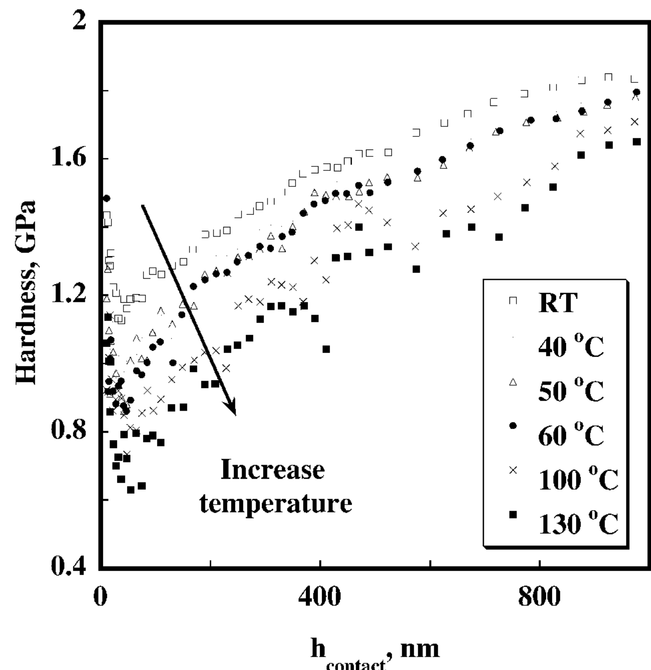

FIG. 6. Hardness as a function of indentation depth for Au films at different testing temperatures.

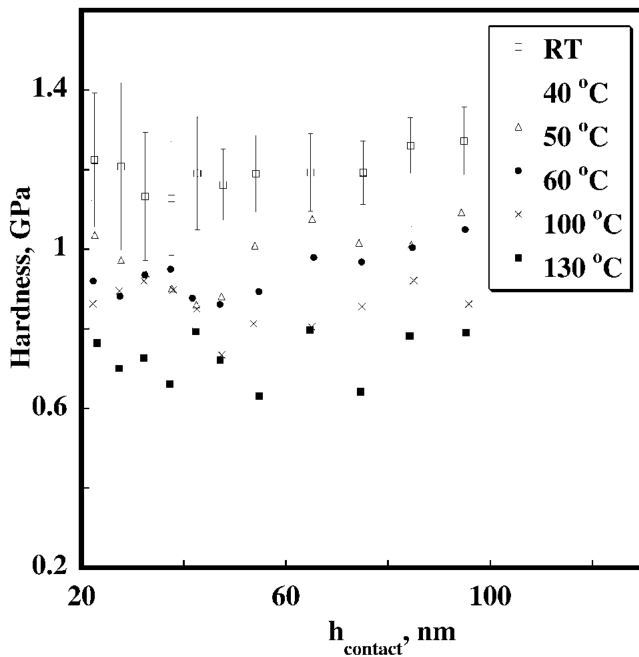

FIG. 7. Shallow indentation-depth hardness-plateau region from Fig. 6.

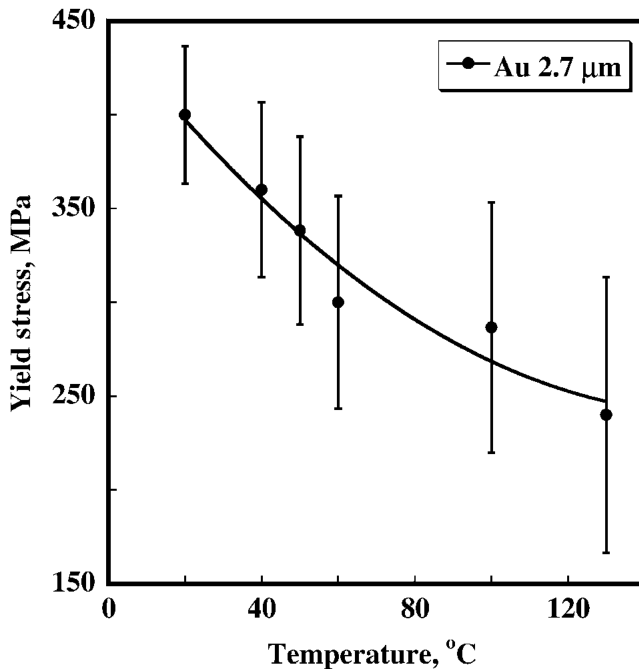

FIG. 8. Yield stress of a 2.7-μm Au film as a function of test temperature.

Tabor relationship (and verified by the inverse method of Eq. (3) for the room-temperature data).

A second-order polynomial provided the best fit to the Au yield stress data over the temperature range tested (Fig. 8). For the 2.7-μm Au film, the yield stress (in MPa) has the following dependence on temperature, T, in Celsius:

$$\sigma_{AuYS}(T) \approx 550 + 0.0112T^2 - 4T \quad . \tag{4}$$

As Cu and Au are both face-centered cubic with similar melting points, we assumed that these nanocrystalline films might have a similar thermal component of the yield stress.[28] Because Cu mechanical properties exhibited a plateau region, similar to Au, we present in Fig. 9 the measurements of Cu film yield stress with a 5-nm Pt overlayer as a function of test temperature. Here, the data are presented with and without thermal drift correction. Thermal drift remained, even though we tried to achieve thermal equilibrium between the indenter tip and the sample by keeping the tip at the sample surface for 2 min before performing indentation experiments. To account for additional drift, the tip was held in contact at 10% of the full load and the tip displacement was measured. The measured thermal drift appeared to be substantial above 60 °C. It was accounted in the final analysis described in the introduction part (I) of this paper by means of adjusting the contact area in the modulus and hardness calculations accordingly.

Besides thermal drift, low-temperature creep is of concern. One may argue that creep effects on elastic modulus at higher loads are substantial, although this effect would result in even higher unloading stiffnesses. Therefore, from the standpoint of creep effects, we are measuring an upper bound for the modulus. Also, is it a true mechanical response of the film that is observed in Fig. 2

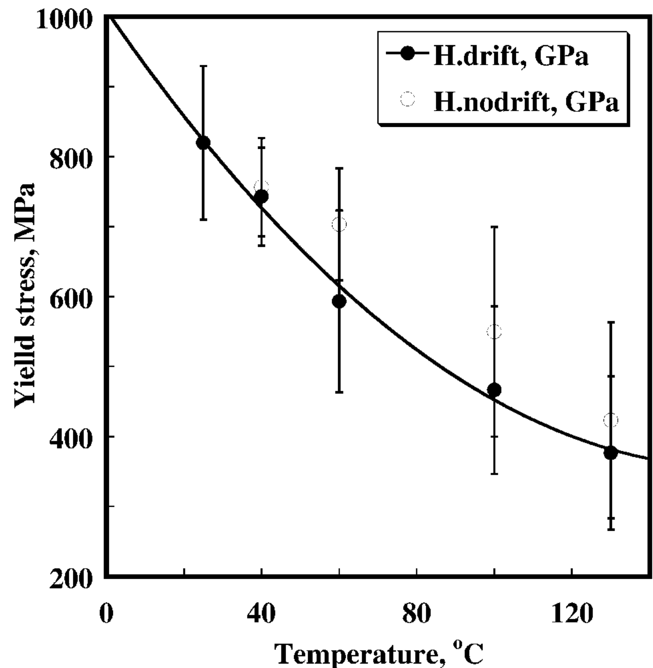

FIG. 9. Yield stress of a 3.2-μm Pt-passivated Cu film as a function of test temperature obtained with and without drift correction.

at the 90% unloading hold, or is it simply a thermal drift? Low temperature plasticity of Cu thin film is given as[27]

$$\dot{\epsilon} = 5.774 \times 10^5 \exp\left[\left(\frac{-2.557 \times 10^4}{T}\right)(1 - 2.177 \times 10^{-9}\sigma)\right] \quad , \tag{5}$$

where $\dot{\epsilon}$ is the strain rate, T is the temperature in Kelvin, and σ is the stress. For the low stress levels of 200 to 300 MPa, the plasticity effects are negligible, giving strain rates from 1.6×10^{-10} to 1.6×10^{-4}, which are negligible compared to the average indentation strain rates of 0.004. The same applies to the low-temperature creep in Cu films given in Ref. 27 as well

$$\dot{\epsilon} = 46.16\left(\frac{\mu}{T}\right)\left[\sinh\left(\frac{458.4\sigma}{\mu}\right)^5 \exp\left(\frac{-2.369 \times 10^4}{T}\right)\right] \quad , \tag{6}$$

where μ is the shear modulus. This drift-correction procedure appears to be a reasonable method for these moderately high-temperature experiments. The method provides reproducible data within the type of error bars indicated in Fig. 9.

It also turns out that our original assumption of a second-order polynomial dependence for Cu yield stress with respect to temperature holds true

$$\sigma_{CuYS}(T) \approx 1000 + 0.025T^2 - 8T \quad . \tag{7}$$

The measured yield stress for this 3.2-μm thick Cu film is twice that of the 2.7-μm Au film. While copper is naturally harder than gold because of its higher modulus, this factor does not appear to be a plausible explanation for the magnitude of the difference. One possibility is the restriction of dislocation motion due to the oxide layer between Cu and Pt films. A second possibility is due to grain-size effects. Figure 10 shows a 3D AFM image for the Cu surface from which grain size was measured. The average grain size for this film is 670 nm, which is almost five times less than the film thickness. Similar results have also been obtained using TEM analysis. This finding is consistent with previous work showing very small grain sizes for sputter-deposited films.[29] Unlike electroplated Cu films, where grains are normally larger than the film thickness after annealing,[30] sputtered films remain nanocrystalline, a fact that explains their elevated yield stress. For these films the grain size [Eq. (2)] controls plasticity, rather than the film thickness [Eq. (3)].

In general, we propose the following temperature dependence for a nanocrystalline fcc metallic thin film

$$\sigma_{YS}(T) = \sigma_0 + AT^2 + BT \quad , \tag{8}$$

where A and B are fitting parameters, and σ_0 is the yield stress value at 0 °C. Employing Eq. (8), Cu yield strength versus temperature curves are constructed for Au and Cu films (Fig. 11).

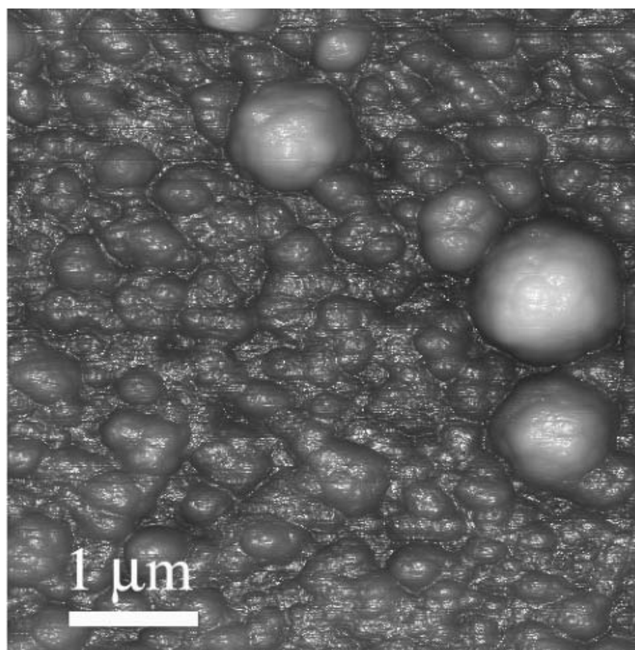

FIG. 10. A 3D AFM image of a 3.2-μm Cu film.

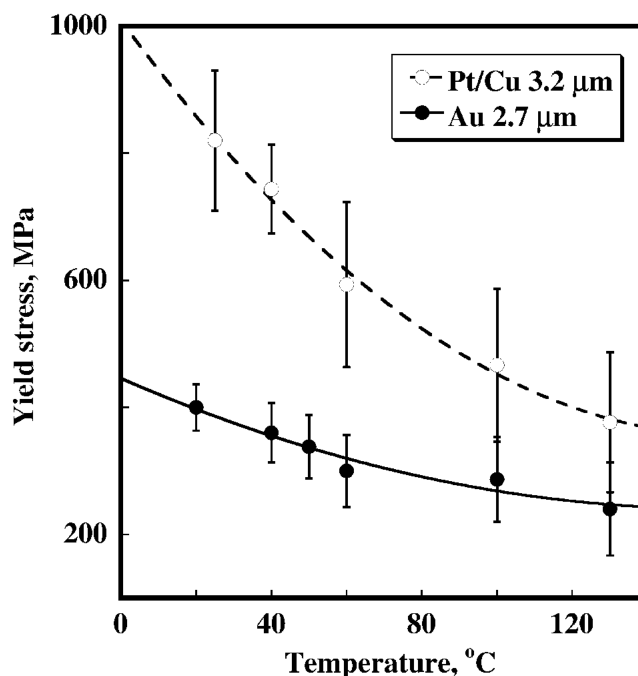

FIG. 11. Yield stress temperature dependence for Cu and Au films.

Although microstructural characterization was not performed after high-temperature nanoindentation, all films were indented before and after high-temperature experiments. The agreement between the hardness values implied no measurable annealing effects.

Temperature effects on the mechanical properties are even more pronounced for softer polymer films.[22,23] Enhanced plasticity typically contributes to the increase in

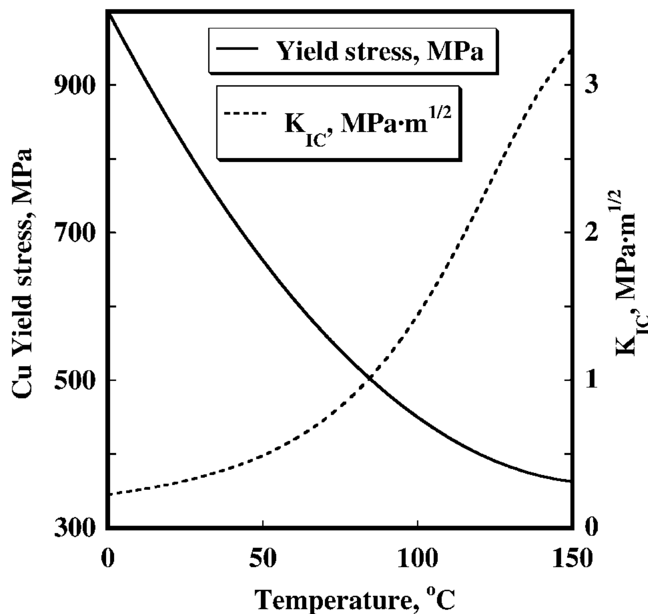

FIG. 12. Interfacial fracture toughness and yield stress for a 3.2-μm Cu film as a function of test temperature.[27]

thin-film adhesion, as more energy is dissipated though plastic deformation than through crack growth.[31,32] In the present case, a reduced copper film yield stress due to the temperature increase assists in an increase of the films' adhesion. Here we will rely on the dislocation-free zone model[28] to provide interfacial fracture toughness predictions for a 3.2-mm Cu film as a function of test temperature. According to the dislocation-free zone model, the interfacial fracture toughness is given by

$$K_I = \frac{1}{A} \exp\left(\frac{B}{\sigma_{ys} c}\right) \quad , \tag{9}$$

where $A = 20$ MPa^{-1}·m$^{-1/2}$, $B = 121$ Pa·m, σ_{ys} is the film yield stress, and c is the dislocation-free zone (80–100 nm for Cu).[28,31] Using Eq. (7) for the Cu yield stress allows constructing Fig. 12 based on Eq. (9). The effects of enhanced plasticity at elevated temperatures in Cu films are also discussed in Refs. 28, 31, and 32.

IV. CONCLUSIONS AND SUMMARY

We have demonstrated the feasibility of high-temperature nanoindentation experiments using a local heating approach and a drift correction up to 130 °C. Nanoindentation at higher temperatures may be possible in the future as the appropriate heating devices become commercially available. A key to developing such a device would be the cooling system, possibly both for the sample and the indenter tip, to ensure the minimal thermal drift.

Both the elastic modulus and yield strength of Au and Cu films were shown to decrease with increasing temperature up to 130 °C. For face-centered-cubic metal films (such as Au and Cu), the yield stress is shown to decrease as a function of temperature, using a second-order polynomial. These small increases in temperature enhance the thin-film interfacial fracture toughness.[28,31,32]

During the preparation of this article, it came to our attention that the elastic modulus decrease of 33% was observed experimentally in free-standing Al thin films tested in tension at temperatures up to 160 °C.[33] The effect is attributed to the anelastic relaxation behavior of nanocrystalline materials due to the softening of grain boundaries at elevated temperatures, which is grain size dependent.[34,35]

ACKNOWLEDGMENTS

The authors would like to acknowledge the support from Sandia National Labs, Livermore, CA. We greatly appreciate the help from Min Li with TEM analysis, and from Megan Cordill (now at the University of Minnesota) with AFM imaging.

REFERENCES

1. D.T. Read and J.W. Dally: A new method for measuring the strength and ductility of thin films. *J. Mater. Res.* **8,** 1542 (1993).
2. T.P. Weihs, S. Hong, J.C. Bravman, and W.D. Nix: Mechanical deflection of cantilever microbeams: A new technique for testing the mechanical properties of thin films. *J. Mater. Res.* **3,** 931 (1988).
3. S.P. Baker and W.D. Nix: Mechanical properties of compositionally modulated Au–Ni thin films: Nanoindentation and microcantilever deflection experiments. *J. Mater. Res.* **9,** 3131, 3145 (1994).
4. G.M. Pharr, D.S. Harding, and W.C. Oliver: *Mechanical Properties and Deformation Behavior of Materials Having Ultra-Fine Microstructures,* in Proceedings of the NATO Advanced Study Institute, edited by M. Nastasi, D.M. Parkin, and H. Gleiter. (Kluwer Academic Publishers, Netherlands, 1993), pp. 449–461.
5. M. Doerner and W.D. Nix: A method for interpreting the data from depth-sensing indentation instruments. *J. Mater. Res.* **1,** 601 (1986).
6. G.M. Pharr, W.C. Oliver, and F. Brotzen: On the generality of the relationship between contact stiffness, contact area, and elastic modulus during indentation. *J. Mater. Res.* **7,** 613 (1992).
7. W.C. Oliver and G.M. Pharr: *J. Mater. Res.* **7,** 1564 (1992).
8. D. Tabor: *The Hardness of Metals* (Claredon Press, Oxford, U.K., 1951) p. 174.
9. D. Kramer, H. Huang, M. Kriese, J. Robach, J. Nelson, A. Wright, D. Bahr, and W.W. Gerberich: Yield strength predictions from the plastic zone around nanocontacts. *Acta Mater.* **47,** 333 (1999).
10. D.E. Kramer, A.A. Volinsky, N.R. Moody, and W.W. Gerberich: Substrate effects on indentation plastic zone development in thin soft films. *J. Mater. Res.* **16,** 3150 (2001).
11. W.D. Nix: Mechanical properties of thin films. *Metal. Trans. A* **20A,** 2217 (1989).
12. Y. Wei and J.W. Hutchinson: Steady-state crack growth and work

of fracture for solids characterized by strain gradient plasticity. *J. Mech. Phys. Solids* **45,** 1137 (1997).
13. H. Inui, M. Matsumuro, D-H. Wu, and M. Yamaguchi: Temperature dependence of yield stress, deformation mode and deformation structure in single crystals of TiAl (Ti-56 at.%Al). *Philos. Mag. A* **75,** 395 (1997).
14. B.N. Lucas and W.C. Oliver: Indentation power-law creep of high-purity indium. *Metall. Mater. Trans. A* **30,** 601 (1999).
15. B.N. Lucas: An experimental investigation of creep and viscoelastic properties using depth-sensing indentation techniques, Ph.D. Dissertation, The University of Tennessee, Knoxville, TN, 1997.
16. E.A. Stach, T. Freeman, A.M. Minor, D.K. Owen, J. Cumings, M.A. Wall, T. Chraska, R. Hull, J.W. Morris, Jr., A. Zettl, and U. Dahmen: Development of a nanoindenter for in-situ transmission electron microscopy and microanalysis. *Microsc. and Microanal.* **7,** 507 (2001).
17. B.D. Beake, and J.F. Smith: High-temperature nanoindentation testing of fused silica and other materials. *Philos. Mag. A* **82,** 2179 (2003).
18. J.F. Smith and S. Zheng: High temperature nanoscale mechanical property measurements. *Surf. Eng.* **16,** 143 (2000).
19. MTS Systems Corporation. Variable temperature nanoindentation (Oak Ridge, TN, 2004). World wide web: http://www.mts.com/nano/Variable_temp.htm.
20. A.A. Volinsky: The role of geometry and plasticity in thin ductile film adhesion, Ph.D. Dissertation, University of Minnesota, Minneapolis, MN, 2000.
21. Thermal Accessory for MultiMode and Dimensions Scanning Probe Microscopes. Support Note No. 252, Rev. B, Digital Instruments, 1998.
22. D. Ivanov, R. Daniels, and S. Magonov: Exploring the high-temperature AFM and its use for studies of polymers. Digital Instruments Application Notes, 2001.
23. X. Xia: Micro/nanoprobing measurement of polymer coating/film mechanical properties, Ph.D. Dissertation, University of Minnesota, 2000.
24. O.D. Sherby: In *Nature and Properties of Materials: An Atomistic Interpretation,* edited by J. Pask (Wiley, New York, 1967) p. 376.
25. L. Burakovsky, C.W. Greeff, and D.L. Preston: Analytic model of the shear modulus at all temperatures and densities. *Phys. Rev. B* **67,** 094107 (2003).
26. S.M. Collard and R.B. McLellan: High-temperature elastic constants of gold single-crystals. *Acta Metall. Mater.* **39,** 3143 (1991).
27. R.P. Vinci, E.M. Zielinski, and J.C. Bravman: Thermal strain and stress in copper thin films. *Thin Solid Films* **262,** 142 (1995).
28. W.W. Gerberich, A.A. Volinsky, N.I. Tymiak, and N.R. Moody: A brittle to ductile transition (BDT) in adhered thin films, in *Thin Films-stresses and Mechanical Properties VIII,* edited by R. Vinci, O. Kraft, N. Moody, P. Besser, and E. Snaffer II (Mater. Res. Soc. Symp. Proc. **594,** Warrendale, PA, 2000). p. 351.
29. N.I. Tymiak, A.A. Volinsky, M.D. Kriese, S.A. Downs, and W.W. Gerberich: The role of plasticity in bi-material fracture with ductile interlayers. *Metall. and Mater. Trans. A* **31A,** 863 (2000).
30. A.A. Volinsky, J. Vella, I.S. Adhihetty, V. Sarihan, L. Mercado, B.H. Yeung, and W.W. Gerberich: Adhesion quantification of post-CMP copper to amorphous SiN passivation by nanoindentation, in *Fundamentals of Nanoindentation and Nanotribiology II,* edited by S.P. Baker, R.F. Cook, S.G. Corcoran, and N.R. Moody (Mater. Res. Soc. Symp. Proc. **649,** Warrendale, PA, 2001) Q 5.3.1.
31. A.A. Volinsky, N.R. Moody, and W.W. Gerberich: Interfacial toughness measurements for thin films on substrates. *Acta Mater.* **50,** 441 (2002).
32. A.A. Volinsky, D.F. Bahr, M.D. Kriese, N.R. Moody, and W.W. Gerberich: Nanoindentation methods in interfacial fracture testing, Chapter 13 in *Comprehensive Structural Integrity,* edited by I. Milne, R.O. Ritchie, and B. Karihaloo, in *Volume 8: Interfacial and Nanoscale Failure,* edited by W.W. Gerberich and W. Yang (Elsevier, New York, 2003).
33. Taher Saif: University of Illinois at Urbana-Champaign, Private Communication.
34. C. Zener, D. van Winkle, and H. Nielson: *Trans. A.I.M.E.* **147,** 98 (1942).
35. Ting-Sui Ke: *Phys. Rev.* **71,** 533 (1947).